APPLIED AND ENVIRONMENTAL MICROBIOLOGY, Feb. 1987, p. 217–223
0099-2240/87/020217-07$02.00/0

Vol. 53, No. 2

Estimation of Bacterial Nitrate Reduction Rates at In Situ Concentrations in Freshwater Sediments

CORNELIS A. HORDIJK, MARCHEL SNIEDER, JOHANNES J. M. VAN ENGELEN, AND THOMAS E. CAPPENBERG*

Limnological Institute, Vijverhof Laboratory, 3631 AC Nieuwersluis, The Netherlands

Received 8 September 1986/Accepted 31 October 1986

A method was developed to follow bacterial nitrate reduction in freshwater sediments by using common high-performance liquid chromatographic equipment. The low detection limit (14 pmol) of the method enabled us to study concentration profiles and reaction kinetics under natural conditions. Significant nitrate concentrations (1 to 27 μM) were observed in the sediment of Lake Vechten during the nonstratified period; the concentration profiles showed a successive depletion of oxygen, nitrate, and sulfate with depth. The profiles were restricted to the upper 3 cm of the sediment which is rich in organics and loosely structured. Nitrate reduction in the sediment-water interface followed first-order reaction kinetics at in situ concentrations. Remarkably high potential nitrate-reducing activity was observed in the part of the sediment in which nitrate did not diffuse. This activity was also observed throughout the whole year. Estimates of K_m varied between 17 and 100 μM and V_{max} varied between 7.2 and 36 μmol cm^{-3} day^{-1} for samples taken at different depths. The diffusion coefficient of nitrate ([10 ± 0.4] $\times 10^{-6}$ cm^2 s^{-1}) across the sediment-water interface was estimated by a constant-source technique and applied to a mathematical model to estimate the net nitrate reduction during the nonstratified period. In this period, observed nitrate reduction rates by the model, 0.2 to 0.4 mmol m^{-2} day^{-1}, were lower than those found for oxygen (27 mmol m^{-2} day^{-1}) and sulfate (0.4 mmol m^{-2} day^{-1}). During the summer stratification, nitrate was absent in the sediment and reduction could not be estimated by the model.

Anaerobic respiration in limnic sediment plays an important role in nutrient remineralization (3). Good insight into the mechanism involving these electron transfer processes is essential for a reliable quantification of the role of sediment in the carbon cycle. Recent studies demonstrated important differences between terminal metabolic pathways in marine and freshwater ecosystems (8, 12). The main difference is the continuous electron acceptor limitation in most freshwater sediments. In most submerged marine sediments electron donor limitation is more likely to occur due to the permanent high sulfate concentration in the water layer above the sediment. Anions that can serve as terminal electron acceptors in freshwater sediments are, in order of net energy yield, oxygen, nitrate, and sulfate. The concentrations of these compounds in the water layer of Lake Vechten showed the typical seasonal fluctuation of a mesotrophic monomictic lake (21). In the summer season stratification occurs, and concentration profiles of oxygen, nitrate, and sulfate (8, 21, 28) in the water phase showed that these electron acceptors were already depleted in the hypolimnion before they could diffuse to the sediment in the deeper parts of the lake. In this season dead organic material, originating from primary production and detritus, deposits in the deeper part of the lake, where it accumulates on the sediment surface. In the nonstratified period complete circulation of the lake occurs, and the electron acceptors diffuse to the deeper parts of the lake. In this period steep concentration profiles of the electron acceptors develop in the sediment, reflecting an equilibrium between transport by diffusion from the overlying water layer and their successive consumption by intense respiration.

Natural nitrate concentrations in marine as well as in most freshwater sediments are low, and analytical tools to measure these low nitrate concentrations are lacking (10, 18). This is one of the reasons why nitrate reduction is generally quantified from the accumulation of ^{15}N-labeled reaction products rather than by directly following nitrate depletion (14, 20). The relevance of the reported rates may be questioned in many cases, since nitrate is generally added at concentrations much higher then those found in nature (13, 18). Sediment enrichment with nitrate might artificially induce zero-order kinetics, normally not occurring in situ. Applying the sensitive and simple ion-chromatographic technique developed during this study enabled us, first, to measure nitrate reduction kinetics in small (5- to 10-ml) sediment batches at in situ concentrations and, second, to estimate nitrate reduction by mathematical modeling. The small sample volumes needed by this technique allow the study of steep, nondisturbed concentration profiles of nitrate essential for quantification by modeling.

MATERIALS AND METHODS

Apparatus. The liquid chromatograph consisted of a model 1330 pump and a model 1305 UV detector (Bio-Rad Laboratories, Richmond, Calif.). Samples were introduced by a Rheodyne 7125 valve with a 50-μl loop. The column (75 by 4.6 mm; HPLC Technology, Cheshire, England) was packed with 5 μm of Nucleosil 5-SB anion-exchange particles. A guard column (75 by 2.1 mm) (type B for anion-exchange chromatography; Chrompack, Middelburg, The Netherlands) was used. The columns were insulated with cotton wool for temperature stability. The eluent was made by diluting sulfuric acid to 1 mM in deionized water filtered through a Milli-Q purification system (Millipore Corp.). The nitrate blank of the Milli-Q water was <0.08 μM (5 ppb). The pH of the eluent was carefully adjusted with NaOH (pH 4.5). The eluent was stored in the dark. Nitrate and nitrite concentrations were evaluated by external standardization.

* Corresponding author.

For calibration, a series of mixtures containing gravimetric standard solutions of nitrate (1.6 to 24 μM [0.1 to 1.5 ppm]) were used. The calibration curves were made by plotting the peak heights obtained from the chromatograms against the concentration of the original standard solutions. In routine analysis, chromatographic peaks were integrated with a combination of an IBM computer and a CI-10 integrator (LDC Milton Roy, Riviera Beach, Fla.).

Sample collection. Undisturbed sediment cores were taken by a modified Jenkin mud sampler from the deepest part of the eastern depression of Lake Vechten (2). The lake is described in detail elsewhere (21). The upper water layer was carefully removed to prevent mixing of the nitrate-rich and oxygen-containing water layer with the nitrate-poor interstitial water of the sediment. Sediment subsamples (1.3 g, wet weight) were drawn by piercing a syringe through the 2-mm holes (covered with Scotch tape [no. 471]) in the acrylic glass sampling tube. The sediment samples were immediately anaerobically transferred into screw-capped vials (Pierce Chemical Co., Rockford, Ill.) and centrifuged at 1,000 × *g* at room temperature for 2 min. The supernatant was separated from the sediment and immediately stored at −20°C upon analysis in small (0.4-ml) polypropylene vials (Tamson, Zoetemeer, The Netherlands). Before analysis, the supernatant was thawed and centrifuged to remove excess organic material by coprecipitation with the formed Fe(III) colloids. A 50-μl portion of the supernatant was injected into the liquid chromatograph for nitrate analysis. For nitrite analysis, the pore water was directly injected under anaerobic conditions. The eluent of the liquid chromatograph was continuously flushed with helium to suppress any nitrite oxidation artifacts and formation of bubbles in the pump head during elution. Sulfate analyses were performed simultaneously by indirect photometric chromatography (6).

Recovery of nitrate. To determine the recovery of nitrate after sampling and centrifugation, sediment was withdrawn from the Jenkin core at −1-cm depth and homogenized. Nitrate reduction was suppressed by gamma radiation (2.5 Mrad) or anaerobic autoclaving (30 min at 125°C) or by adding Halamid (final concentration, 4%). The inactivated slurry was divided into five batches of 10 ml each, which were spiked with nitrate to obtain a standard series with final concentrations in the pore water of 0 to 64 μM nitrate. The batches were incubated anaerobically in the dark at 8°C. Subsamples were withdrawn after 15 h of incubation. Nitrate concentration series in the pore water were curve compared with gravimetric standard series made in distilled water. The recovery was calculated from the ratio of the slopes of both calibration curves made from the plots of peak height against concentration. Nitrate recovery in aerated sediment was determined in the same way. The slurry was, however, not deactivated but flushed overnight with air. The sediment batches were spiked with nitrate (16 to 64 μM) and shaken under air for 3 h. In between, subsamples were taken from each batch for nitrate analyses. The slope of the obtained calibration curve made in the sediment was compared with that made in distilled water to estimate the recovery.

Sediment characterization. Sediment samples were collected at different depths of the Jenkin core as mentioned and centrifuged in calibrated (1.3-ml) reaction vials (Pierce) at 1,000 × *g*. The pore water was withdrawn for nitrate and sulfate analyses. The remaining sediment was dried at 110°C to determine the dry weight per milliliter of wet sediment. Nitrogen and carbon per milliliter of wet sediment were measured with a CHN-analyzer (model 240; The Perkin-Elmer Corp., Norwalk, Conn.) (28). Redox potential and oxygen measurements were done by dipping microelectrodes into the Jenkin core at 1-mm intervals (16).

Model of NO_3^- dynamics. The model applied to estimate nitrate reduction is derived from the one used by Berner (1) to estimate sulfate reduction in marine sediments. The basic assumption of the model is that the concentration change of nitrate with time at a given depth x is a reflection, mainly, of three processes: (i) diffusion according to Fick's second law; (ii) deposition; (iii) nitrate reduction.

$$\left.\frac{\partial C}{\partial t}\right|_x = D_s \frac{\partial^2 C}{\partial x^2} - \omega \frac{\partial C}{\partial x} - f(x) \quad [1]$$

In this equation C is the nitrate concentration measured in situ, D_s ($=D_{NO_3}$) is the diffusion coefficient, ω is the rate of sedimentation in Lake Vechten (1.8×10^{-3} cm day^{-1} [22]), and $f(x)$ is a function describing the nitrate reduction at depth x. The definition of this function $f(x)$ depends on the reaction kinetics of nitrate reduction in the sediment-water interface. Assuming that nitrate reduction is limited by diffusion means that first-order kinetics is to expected and the rate of nitrate reduction at depth x will be correlated with the concentration at this depth: $d[NO_3]_x/d_t = -K \cdot [NO_3]_0$ or after intergration, $\ln [NO_3]_t = -K \cdot t \cdot \ln[NO_3]_0$. From this equation we can derive that nitrate reduction will decrease exponentially with depth or

$$f(x) = a \cdot e^{-b(x)} \quad [2]$$

in which x represents the depth in the sediment; a and b are unknown constants. Solving these constants will reveal a function from which at each depth nitrate reduction can be calculated. Under steady-state conditions D_{NO_3} and $f(x)$ are independent of time and $dC/dt = 0$ at depth x. According to Berner (1) and with the border conditions of $C = C_0$ at $x = 0$ and $C = C_\infty$ at $x = \infty$, two solutions can be obtained for differential equation 1

$$C_{(x)} = \frac{a}{D_{NO_3} \cdot b^2 + \omega \cdot b} \cdot e^{-b(x)} + C_\infty \quad [3]$$

$$C_{(x)} = (C_0 - C_\infty) \cdot e^{-bx} + C_\infty \quad [4]$$

where C_0 is the nitrate concentration of the overlying water layer and C_∞ is the minimum nitrate concentration. The a term of function $f(x)$ can be found by substitution of solution 3 in equation 4. The b term of function $f(x)$ can be estimated by fitting computer-generated plots of solution 4 on natural measured nitrate concentration profiles. Nitrate reduction can now be estimated by substitution of a and b terms in function $f(x)$ and successive integration, yielding the practical formula

$$\int_{x_1}^{x_2} f(x)dx = -(C_0 - C_\infty)(\omega + D_s b)e^{-b)x_2 - x_1)} \quad [5]$$

Determination of diffusion coefficient. The model requires an independent estimate of D_{NO_3}, which was determined by the constant-source technique of Duursma and Hoede (4). We previously applied this technique to estimate the diffusion constant of sulfate and proved its realibility by comparison with an instantaneous-source technique (4) and intact whole-core incubations (8). To estimate D_{NO_3}, subcores were filled with 4 cm of inactivated sediment collected from the upper 2 cm of the Jenkin core with a porosity of 0.9. A water layer of 15 cm containing 160 μM NO_3^- was carefully placed above the sediment, and the subcore was incubated at

8°C. Incubation times were carefully optimized until a pure diffusion profile was formed within ±2 cm of sediment. The overlying water layer was occasionally mixed with care to maintain a constant concentration above the sediment. After incubation, the sediment pore water was sampled at 0.5-cm intervals and analyzed for nitrate. The diffusion constant D_{NO_3} was determined by plotting the nitrate concentration against the depth on an error function graph (4).

Sediment slurry incubations. For better insight into the kinetics at the sediment-water interface, subsamples (8 ml) were anaerobically collected at −0.75 cm, using the Jenkin core, and transferred into 20-ml serum vessels. The serum vessels were capped with butyl rubber stoppers and the headspace was flushed with oxygen-free nitrogen. The sediment batches were spiked with nitrate until two or three times the natural concentration and anaerobically incubated at the in situ temperature (8°C) of the sediment. No pH change was observed during incubation. Six subsamples were withdrawn by piercing the syringe through the butyl rubber stopper at 5-min intervals, immediately centrifuged (30 s at 1,000 × *g*), and analyzed or frozen and stored. Instead of serum vessels, 10-ml plastic syringes were also applied for short-term incubation.

RESULTS

Nitrate analysis. We compared the sensitivity of several detection modes in combination with a relatively inexpensive, high-capacity Nucleosil 5-SB anion-exchange column (Table 1). The application of a strong high-capacity column excluded conductometric detection (6, 7). Nonsuppressed conductometric detection with low-capacity columns and indirect photometric detection proved too insensitive (detection limit, <200 pmol [6]), with injection volumes below 100 μl. Direct UV detection with methane sulfonic acid as eluent (9) yielded a detection limit of 80 pmol. Detection limits significantly improved (15 pmol) by replacing methane sulfonic acid with pure sulfate as eluent (pH 4.5) in a concentration range of 0.5 to 2.5 mM. Stable base lines were obtained within 2 h of flushing the column (Fig. 1).

Nitrate and nitrite were well separated at an eluent concentration of 1 mM H_2SO_4 (nitrate retention time, 10 min; nitrite retention time, 7 min), without interference of sulfate, thiosulfate, thionate, sulfide, sulfite, or a dissolved organic carbon pool (DOC). Calibration curves were linear between 1.6 and 65 μM (0.1 to 1.4 ppm) with a 50-μl loop (*r*, 0.999) and peak-height measurements. The linearity improved about twofold with electronic integration. The sensitivity of the nitrate analysis is proportional to the volume injected. With 300-μl injections, linear calibration curves for nitrate or nitrite in the range of 0.16 to 1.6 μM (10 to 100 ppb; *r*, 0.999) can be obtained with ease. However, nonpurified pore water injections of this size quickly poison the analytical column head. The analytical column could be used for at least 1,000 analyses within 0.5 year with 50-μl injections. Sequential 50-μl injections of an 8 μM nitrate solution yielded a standard error of 8% with peak-height measurements. An absolute detection limit of 20 pmol was calculated from three times the noise of the detector (1.5×10^{-4} absorbance units full scale) divided by the sensitivity (13.4 absorbance units full scale μmol^{-1}). Standard addition of nitrate to the sample matrix indicated a recovery of 98 ± 2% for both the aerobic and the anaerobic parts of the sediment. Nitrate concentrations did not increase when sediment slurries were mixed under air for 1 h.

TABLE 1. Comparison of different ion chromatographic techniques for nitrate determination, using optical detection

Eluent[a]	Retention time (min)	Molar response (AUFS μmol^{-1})[b]	Detection limit (pmol)
0.4 mM SIPA	4	1.0	200
10 mM MSA	9	5.0	80
0.5 mM H_2SO_4	14	8.1	25
2.5 mM H_2SO_4	8	15.6	15

[a] SIPA, sulfoisophthalic acid; MSA, methane sulfonic acid.
[b] AUFS, Absorbance units full scale.

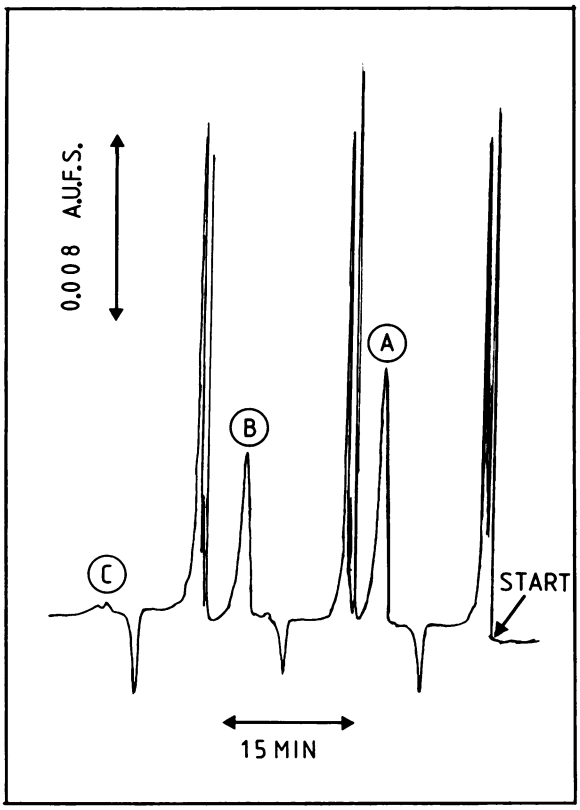

FIG. 1. Nitrate chromatograms of sedimental pore water. Samples were taken in the nonstratified period at 0 (A), −0.5 (B), and −1.0 (C) cm. Concentrations: A, 27.5 μM; B, 17 μM; C, 1.9 μM. Conditions: Range, 0.04 absorbance units full scale (AUFS); loop, 50 μl; eluent, 0.75 mM H_2SO_4 (pH 4.5); flow rate, 0.8 ml min^{-1}; wavelength, 204 nm.

Field observations. The concentrations of oxygen, nitrate, and sulfate in the deeper parts of Lake Vechten showed the typical seasonal fluctuations of a mesotrophic monomictic lake (21) (Table 2). The highest concentrations of nitrate (25 μM) and sulfate (220 μM) in the water layer just above the sediment were observed in winter and early spring (Table 2), and the lowest concentrations (nitrate, <1 μM; sulfate, <20 μM) were seen at the end of the summer stratification. In the summer no nitrate or nitrite could be detected in the sediment. In the upper 2 cm of sediment there was clearly a successive depletion with depth of oxygen, nitrate, and sulfate in the time that the lake underwent complete circulation (Fig. 2a). Other anions which could serve as potential electron acceptors such as nitrite, sulfite, thiosulfate, or tetrathionate were not found in the sediment. Dry weight (Fig. 2d) frequently increased rather steeply from 50 g dm^{-3}

TABLE 2. Seasonal fluctuation of oxygen, nitrate, and sulfate concentrations in the water layer 1 m above the sediment surface in the lowest part of the eastern depression of Lake Vechten

Fluctuation of:	Concn (μM) in:											
	Jan.	Feb.	Mar.	Apr.	May	June	July	Aug.	Sept.	Oct.	Nov.	Dec.
Oxygen	360	340	340	350	250	0	0	0	0	0	238	375
Nitrate	21	21	20	20	18	0	0	0	0	0	7	11
Sulfate	210	200	200	200	140	80	20	10	10	200	200	200

at the surface of the sediment to 200 g dm^{-3} (at −3 cm). Redox potential (Fig. 2c) dropped sharply, i.e., 170 mV in the upper 4 mm of the sediment and 280 mV at −2.5-cm depth. Note that absolute redox potentials are difficult to estimate as the dissolved iron in the pore water interferes with calibration with the normal electrode. The percentages of N and C in the total dry weight were a little higher in the top layer (Fig. 2b) compared with those in the deeper layers, but the absolute amount of carbon increased from 0.3 M at −0.5 cm to 1.1 M at −3 cm and total N increased from 33 mM at −0.5 cm to 74 mM at −3-cm depth.

Reaction kinetics. Nitrate addition to the sediment collected from the sediment-water interface at −1 cm resulted in a complete nitrate depletion within 0.5 h (Fig. 3). Plots of incubation time versus nitrate concentration on a linear (Fig. 3a) or logarithmic (Fig. 3b) scale showed a shift from zero- to first-order kinetics when the surplus of added nitrate was consumed up until natural concentrations were reached. Intensive nitrate reduction was observed in the sediment during the whole year, including the summer stratification when nitrate is absent in the deeper layers of the lake. Nitrate reduction was also observed in the deeper layers of the sediment. V_{max} decreased with depth from 20.0 (−1 cm) to 18.7 (−3 cm) to 8.4 (−5 cm) to 6.0 (−8 cm) μM day^{-1}. Michaelis-Menten plots were made to estimate when nitrate-reducing rates became concentration dependent. K_m esti-

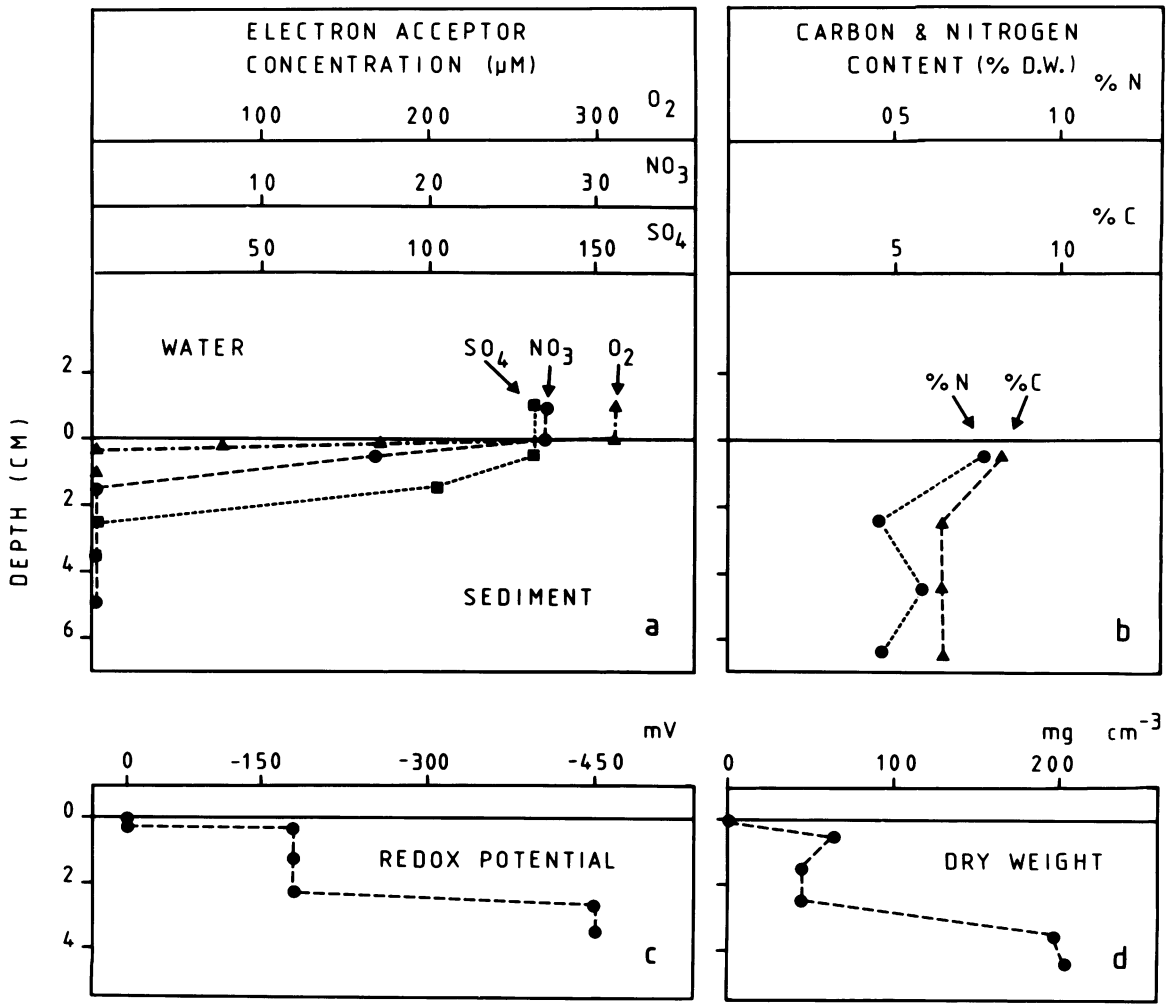

FIG. 2. Concentration profiles at the sediment-water interface of Lake Vechten during the circulation period. (a) Electron acceptors: oxygen (▲); nitrate (●); sulfate (■). (b) Carbon and nitrogen content as percent dry weight. (c) Redox potential. (d) Dry weight. The oxygen and redox potential were measured at 1-mm interval.

mates were 17 (−1 cm), 26 (−1 cm), and 110 (−2 cm) μM in the nonstratified period and 26 μM (−1 cm) during stratification. Figure 4 shows a Michaelis-Menten plot made with the values from Fig. 3a.

Model calculations. The estimated diffusion coefficient of nitrate (D_{NO_3}) in the sediment-water interface was 10.1 ± 0.4 × 10^{-6} cm^2 s^{-1}. The D_{NO_3} values were simular for anaerobic autoclaved, radiated, or Halamid-inactivated sediment. The latter suppressed nitrate reduction only temporarily. In the diffusion experiments, nitrate concentrations in sediment incubated simultaneously remained constant with Halamid as the suppressor. The estimated D_{NO_3} values were comparable to literature values measured in distilled water (15) if corrected for temperature (8°C) and porosity (±0.9). No literature values of D_{NO_3} at the sediment-water interface are known to us. Application of the model to concentration profiles in the circulation period, using the estimated D_{NO_3}, yielded a maximum net reduction rate of 0.3 ± 0.1 mmol m^{-2} day^{-1} (n = 5). The model could not be applied during summer stratification while nitrate is absent in the sediment and in the water layer above the sediment.

DISCUSSION

Nitrate analysis. As in many other Dutch freshwater lakes, the concentration of DOC such as humic acids and other organic compounds in Lake Vechten is high. DOC values vary between 4 and 6 mg of C $liter^{-1}$ in open water and between 12.5 and 15.5 mg of C $liter^{-1}$ in pore water (after filtration through a 0.45-μm filter [3]). For a direct measurement at low-UV wavelengths, the nitrate peak had to be separated well from other UV-absorbing interfering substances present in the DOC pool. A high-capacity column like the Nucleosil 5-SB is capable of separating nitrate from high amounts of organics without overloading. The DOC pool did not interfere with nitrate analysis due to the low affinity of these compounds at low pH for the silica-based anion-exchange column. The DOC pool cannot compete well with the sulfate buffer on the ion-exchange sites of the column, and most of this pool is flushed directly through the column with the void volume. The nitrate anion interacts intensively with the column material and a well-shaped peak evolves. Injection of nonpurified samples into the liquid chromatograph, however, induces a quick decline (1 month) in the column performance by an irreversible absorption of a small part of the DOC pool on the column head with each injection. The column deteriorates; its resolution decreases, dissolution of the column head occurs, and back pressure increases. When large injection volumes (1 to 2 ml) were applied to compensate for insensitive detection, natural profiles were disturbed.

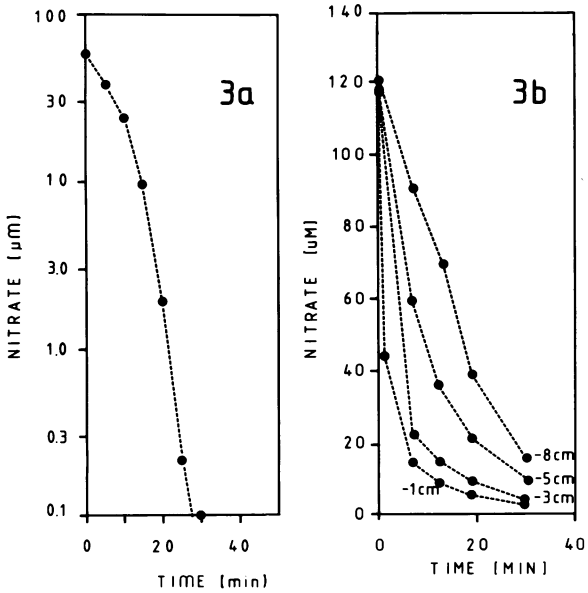

FIG. 3. Semilog plot of nitrate depletion in an 8-ml sediment batch taken at −1-cm depth of the Jenkin Core in the nonstratified period (a) and linear plots of nitrate depletion during the summer stratification at various depths in the sediment (b).

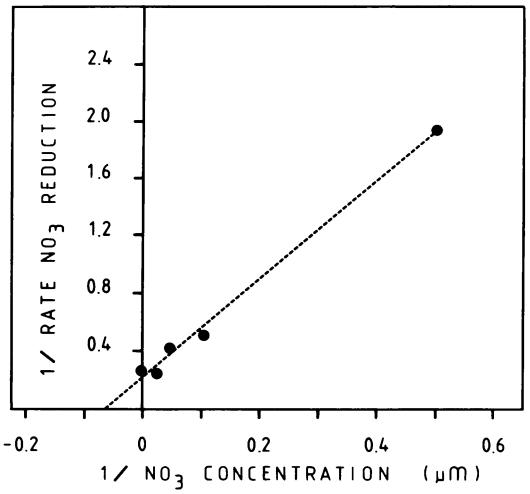

FIG. 4. Lineweaver-Burk plot of nitrate reduction rate as a function of nitrate concentration in the sediment of Lake Vechten. Units of 1/V are given in minutes $micromole^{-1}$ $liter^{-1}$.

The procedure in this paper circumvents most of these difficulties, first, by improving the detection limit, allowing smaller injection volumes (<50 μl) which reduced the amount of DOC brought onto the column; and second, by applying a sample purification procedure, Sample clean-up of organic-rich pore water can be done by eluting the pore water through an absorption column (25). This technique is inconvenient for sample sizes of <200 μl as, although dead volumes can be minimized, the pore water dilutes during elution though the absorption column and must be reconcentrated after collection. A much simpler way of purifying pore water is by slowly freezing out. The DOC pool concentrates and reacts easier in this way with the dissolved Fe(III) present in the pore water. Excess Fe(III) in the pore water is formed by the oxidation of dissolved $Fe(II)CO_3$ (free dissolved Fe pool = 3.6 mM [27]). After thawing, the humic acids and dissolved Fe(III) complexes can be coprecipitated by centrifugation.

Reaction kinetics. Nitrate addition to the sediment immediately stimulates an intensive nitrate-reducing activity. In aerated sediments, however, complete nitrate reduction did not occur until all oxygen was consumed. These experiments together with the observation of steep nitrate concentration profiles indicate that, in the organic-rich sediment of Lake Vechten, nitrate limitation occurs, which restricts respiratory nitrate reduction to a small zone immediately below the oxidized surface. It was remarkable that nitrate reduction was also stimulated immediately by addition of nitrate to deeper parts of the sediment (Fig. 3b) where, in situ, no nitrate was detected. The origin of this potential nitrate-

reducing activity is unknown to us, but simular observations were noted for other sediments (17, 23). Nitrate-reducing activity also occurred during the summer stratification immediately after nitrate addition to the sediment. At this time nitrate was already absent for several months in the eastern depression of the lake (Table 2), implying that an active nitrate-reducing flora is permanently present in the sediment. A nutrical need for assimilatory nitrate reduction is superfluous regarding the amount of NH_4^+ present in the sediment (0.025% of the dry weight [20, 26]), and nitrate reduction in the sediment may therefore be entirely dissimilatory, including the deeper parts of the sediments. We previously also observed a potential sulfate-reducing activity in deeper parts of the sediment (8) in which sulfate no longer diffused.

The reaction kinetics of the nitrate reduction was studied directly by following its depletion in the sediments as no chemical absorption of ntirate was observed in the controls. The lack of significant nitrification was remarkable and agrees with the results of van Kessel (24) that at low temperatures (±4°C) no or little growth of nitrifying bacteria occurs. Potential nitrate-reducing activity decreased with depth, so batch sizes had to be kept to a minimum to prevent mixing up the top layer with less active sediment. Semilogarithmic (Fig. 3a) and linear (Fig. 3b) plots indicated that in enriched sediments nitrate reduction initially follows zero-order kinetics up to natural concentrations, with a sequential shift to first-order kinetics until nearly complete depletion is reached. The K_m values obtained from Michaelis-Menten plots (Fig. 4) varied between 17 and 100 μM and are comparable to those found by Oremland et al. (17) in a marine estuary. Estimation of K_m values or turnover rates requires about 6 ml of sediment as a time course had to be made, and one subsample is needed for each time interval. Taking the steep concentration profiles into account, it cannot be excluded that some mixing of the sediment, even with this sample size, might occasionally occur and influence a precise estimate of K_m or V_{max} values. More important, however, is that mixing the sediment with nitrate excludes the in situ existing limitation by diffusion, which complicates interpretation of the measured reduction rates. Estimation of the actual nitrate reduction by modeling may, therefore, be more reliable than estimations obtained from incubation of slurried sediment batches.

Modeling. The increase of dry weight at ±3-cm depth observed in many Jenkin cores indicates that the sediment-water interface is less consolidated than the layer below. The lack of redox potential fluctuations at millimeter intervals in the sediment-water interface indicates the absence of microniches as reported in marine sediments (11). The similar C/N ratios found in the sediment and the sediment-water interface also indicate a homogeneous structure, ideal for mathematical modeling. In Lake Vechten sediment, respiration processes were found to be restricted to the loosely bound sediment-water interface as methanogenesis mainly occurs in the more compact layer (Fig. 2d) marked by the sharp decrease in redox potential (Fig. 2c). The steep concentration profiles of the investigated electron acceptors (Fig. 2a) are obviously a reflection of a steady state between an intensive reduction and diffusion. Their successive depletion with depth might be explained by the net energy yield of the involved electron transfer processes (19). For example, the energy yield gained by the oxidation of acetate, an important potential electron donor (5), is much higher with the reduction of oxygen (27 kcal [113 kJ] electron mol^{-1}) or nitrate (17 kcal [71 kJ] electron mol^{-1}) than with that of sulfate (3 kcal [13 kJ] electron mol^{-1}). Nitrate reduction apparently outcompetes sulfate reduction in the anaerobic zone.

Applying the model with the estimated diffusion coefficient ($D_{NO_3} = 10.10^{-6}$ cm^2 s^{-1}) yielded a nitrate reduction of 0.3 ± 0.1 mmol m^{-2} day^{-1}, a rate much lower than the potential nitrate reduction rate expected for batch experiments (±74 mmol m^{-2} day^{-1}). The latter was estimated by the formula $v = V_{max} \cdot C/(K_m + C)$ given by Oren and Blackburn (18), in which v is the nitrate reduction rate, C is the mean nitrate concentration at −1 cm, and K_m is the Michaelis-Menten constant from Fig. 4. The estimated nitrate reduction by the model is in the same range as the simultaneously estimated sulfate reduction (0.4 mmol m^{-2} day^{-1}) but much lower than the estimated oxygen consumption (±27 mmol m^{-2} day^{-1}). More information is needed to translate these numbers in terms of carbon mineralization throughout the whole year because internal remineralization processes (especially for sulfate) in the sediment are not taken into account by the model.

ACKNOWLEDGMENTS

We thank our colleagues Herb L. Fredrickson and Ramesh D. Gulati for helpful manuscript reviews. We also thank H. L. Lindeboom (Delta Institute for Hydrobiological Reseach, Yerseke, The Netherlands) for the microelectrode measurements, H. Roon for assistance in the field, and E. M. Marien for photography.

LITERATURE CITED

1. **Berner, R. A.** 1964. An idealized model of dissolved sulfate distribution in recent sediments. Geochim. Cosmochim. Acta **28**:1497–1503.
2. **Cappenberg, T. E.** 1974. Interrelations between sulfate-reducing and methane-producing bacteria in bottom deposits of a freshwater lake. I Field observations. Antonie van Leeuwenhoek J. Microbiol. Serol. **40**:285–295.
3. **Cappenberg, T. E., and H. Verdouw.** 1982. Sedimentation and breakdown kinetics of organic matter in the anaerobic zone of Lake Vechten. Hydrobiologia **95**:165–195.
4. **Duursma, E. K., and C. Hoede.** 1967. Theoretical, experimental and field studies concerning molecular diffusion of radio isotopes in sediments and suspended solid particles of the sea. Neth. J. Sea Res. **3**:423–457.
5. **Hordijk, C. A., and T. E. Cappenberg.** 1983. Quantitative high-pressure liquid chromatography-fluorescence determination of some important lower fatty acids in lake sediments. Appl. Environ. Microbiol. **46**:361–369.
6. **Hordijk, C. A., and T. E. Cappenberg.** 1985. Sulfate analysis in pore water by radio-ion chromatography employing 5-sulfoisophthalic acid as a novel eluent. J. Microbiol. Methods **3**: 205–214.
7. **Hordijk, C. A., C. P. C. M. Hagenaars, and T. E. Cappenberg.** 1984. Analysis of sulfate at the mud-water interface of freshwater lake sediments using indirect photometric chromatography. J. Microbiol. Methods **2**:49–56.
8. **Hordijk, C. A., C. P. C. M. Hagenaars, and T. E. Cappenberg.** 1985. Kinetic studies of bacterial sulfate reduction in freshwater sediments by high-pressure liquid chromatography and microdistillation. Appl. Environ. Microbiol. **49**:434–440.
9. **Ivey, J. P.** 1983. Novel eluent for the UV and conductometric detection of anions in unsuppressed ion chromatography. J. Chromatogr. **267**:218–221.
10. **Jones, J. G., and B. M. Simon.** 1981. Differences in microbial decomposition processes in profundal and littoral lake sediments, with particular reference to the nitrogen cycle. J. Gen. Microbiol. **123**:297–312.
11. **Jørgensen, B. B.** 1978. A comparison of methods for the quantification of bacterial sulfate reduction in coastal marine sediments. I. Measurement with radiotracer techniques. J.

Geomicrobiol. **1**:11–27.
12. **Jørgensen, B. B.** 1985. Seasonal cycles of O_2, NO_3^- and SO_4^{2-} reduction in estuarine sediments; the significance of an NO_3^- reduction maximum in spring. Mar. Ecol. Prog. Ser. **24**:65–74.
13. **Kaspar, H. F.** 1982. Denitrification in marine sediment: measurement of capacity and estimate of in situ rate. Appl. Environ. Microbiol. **43**:522–527.
14. **King, D., and D. B. Nedwell.** 1985. The influence of nitrate concentration upon end products of nitrate dissimilation by bacteria in anaerobic salt marsh sediment. FEMS Microbiol. Ecol. **31**:23–28.
15. **Lerman, A.** 1979. Diffusion coefficients in solution, p. 79–100. *In* A. Lerman (ed.), Geochemical processes in water and sediment environments. John Wiley & Sons, Inc., New York.
16. **Lindeboom, H. J., and A. J. J. Sandee.** 1985. A new bell jar/microelectrode method to measure changing oxygen fluxes in illuminated sediments with a microalgal cover. Limnol. Oceanogr. **30**:693–698.
17. **Oremland, R. S., C. Umberger, C. W. Culbertson, and R. L. Smits.** 1984. Denitrification in San Francisco Bay intertidal sediments. Appl. Environ. Microbiol. **47**:1106–1112.
18. **Oren, A., and T. H. Blackburn.** 1979. Estimation of sediment denitrification rates at in situ nitrate concentrations. Appl. Environ. Microbiol. **37**:174–176.
19. **Peck, H. D., and J. LeGall.** 1982. Biochemistry of dissimilatory sulfate reduction. Philos. Trans. R. Soc. London Ser. B **298**: 443–466.
20. **Sørensen, J.** 1978. Capacity for denitrification and reduction of nitrate to ammonia in a coastal marine sediment. Appl. Environ. Microbiol. **35**:305–310.
21. **Steenbergen, C. L. M., and H. Verdouw.** 1982. Lake Vechten: aspects of its morphometry, climate, hydrology and physicochemical characteristics. Hydrobiologia **95**:11–23.
22. **Steenbergen, C. L. M., and H. Verdouw.** 1984. Carbon mineralization in microaerobic and anaerobic strata of Lake Vechten (The Netherlands): diffusion flux calculations and sedimentation measurements. Arch. Hydrobiol. Beih. Ergebn. Limnol. **19**: 183–190.
23. **Tiedje, J. M., A. J. Sexstone, D. D. Myrold, and J. A. Robinson.** 1982. Denitrification: ecological niches, competition and survival. Antonie van Leeuwenhoek J. Microbiol. Serol. **48**:569–583.
24. **van Kessel, J. F.** 1977. Factors affecting the denitrification rate in two water-sediment systems. Water Res. **11**:259–267.
25. **Varga, G.M., I. Csiky, and J. A. Jonsson.** 1985. Ion chromatographic determination of nitrate and sulfate in natural waters containing humic substances. Anal. Chem. **56**:2066–2069.
26. **Verdouw, H., P. C. M. Boers, and E. M. J. Dekkers.** 1985. The dynamics of ammonia in sediments and hypolimnion of Lake Vechten (The Netherlands). Arch. Hydrobiol. **105**:79–92.
27. **Verdouw, H., and E. M. J. Dekkers.** 1980. Iron and manganese in Lake Vechten (The Netherlands); dynamics and role in the cycle of reducing power. Arch. Hydrobiol. **89**:509–532.
28. **Verdouw, H., and E. M. J. Dekkers.** 1982. Nitrogen cycle of Lake Vechten: concentration patterns and internal mass-balance. Hydrobiologia **95**:191–197.